Holography of particle tracks in the Fermilab 15-Foot Bubble Chamber

E-632 Collaboration *

H. Bingham and J. Lys
University of California, Berkeley, CA 94720, USA

L. Verluyten [1,10] and S. Willocq [2]
Interuniversity Institute for High Energies (ULB-VUB), B-1050 Brussels, Belgium, and Fermilab, Batavia, IL 60510, USA

J. Moreels
Interuniversity Institute for High Energies (ULB-VUB), B-1050 Brussels, Belgium

K. Geissler, G.G. Harigel and D.R.O. Morrison
CERN, CH-1211 Geneva 23, Switzerland

F. Bellinger [3], H. Bjelkhagen [4], H. Carter, J. Ellermeier, J. Foglesong, J. Hawkins, J. Kilmer, T. Kovarik, W. Smart, J. Urbin, L. Voyvodic, E. Wesly [5] and W. Williams
Fermilab, Batavia, IL 60510, USA

R.J. Cence and M.W. Peters
University of Hawaii, Honolulu, HI 96822, USA

R.A. Burnstein and R. Naon
Illinois Institute of Technology, Chicago, IL 60616, USA

P. Nailor [6]
Imperial College, London SW7, UK

M. Aderholz
Max-Planck-Institut für Physik und Astrophysik, D-8000 München 40, FRG

G. Corrigan [7]
University of Oxford, Oxford OX1 3RH, UK

R. Plano

Rutgers University, New Brunswick, NJ 08903, USA

R.L. Sekulin and S. Sewell [8]

Rutherford Appleton Laboratories, Didcot OX11OQX, UK

E.B. Brucker

Stevens Institute of Technology, Hoboken, NJ 07030, USA

H. Akbari [9], R.H. Milburn, D. Passmore and J. Schneps

Tufts University, Medford, MA 02155, USA

During a quadrupole–triplet neutrino experiment with the 15-Foot Bubble Chamber at Fermilab, a large number of events was recorded on ~110000 good holograms, which were taken simultaneously with the conventional three-view photographs. The holograms allow the study of event vertices in a large volume with greatly improved resolution. The experimental setup and the operation of the system is described. Preliminary results obtained during the replay of holograms with the newly developed real- and virtual-image machines are discussed.

1. Introduction

Holography offers the possibility of photographing large volumes with better resolution than obtainable with conventional optics. This is of particular interest for the study of elementary particle interactions in gaseous or liquid detectors, where one searches for rare interactions with short lifetimes (i.e. short track lengths). The feasibility of this technique had been demonstrated for the first time in a 120-cm^3 bubble chamber (Berne Infinitesimal Bubble Chamber BIBC [1]). The exposure of a 2 l chamber (Holographic Bubble Chamber HOBC [2]) in a hadron beam at CERN resulted in 40000 holograms, which were analyzed. However, bubble chambers operated in neutrino beams are the most useful applications of this technique [3,4]. In the large cryogenic bubble chambers [3] the aim is to holograph bubbles in a volume of up to several cubic meters ~ 1 ms after their creation, when they have grown to only ~ 100 μm in diameter. These holograms supplement the conventional stereophotographs of particle tracks taken some ten milliseconds later, when the bubbles have grown to diameters of ~ 400 μm. These two techniques combine the advantages of a quick overall view, easy event recognition and track measurement in the conven-

tional photographs, with the more detailed picture of the interesting event vertex region in the holograms.

The present paper describes the experience with holography in the 15-Foot Bubble Chamber at Fermilab, gained during a technical run (1984) and two physics runs (1985 and 1987/88). The Chamber was exposed to a quadrupole-triplet neutrino beam with 800 GeV/c protons from the Tevatron on the production target. In the second physics run, 293060 conventional 3-view pictures and ~ 218000 holograms, of which ~ 110000 are useful for physics analysis, were recorded simultaneously. The analysis of these photographs and holograms is in progress and some preliminary results from the scanning of the holograms will be presented.

We limit ourselves here to a description of the modified single-beam holography. The basic idea had been developed by C. Baltay of Columbia University [3,5] and was tested earlier in the Big European Bubble Chamber (BEBC) at CERN [6,7]. First results from its application in the 15-Foot Bubble Chamber can be found in refs. [8–11]. The main emphasis of this paper is on the technical aspects of the layout used in the second physics run and on the practical experience with this system. Descriptions of replay machines built for the analysis of these holograms are given in refs. [12–15]. Features of two-beam illumination systems for large volume holography can be found in ref. [16].

In section 2, we describe the theory and design considerations of our modified single-beam technique, with emphasis on the layout of the illumination system, its adaption to the existing geometry of the 15-Foot Bubble Chamber, and on a variety of effects due to

---

[8] Now with Autofile Ltd., Slough, UK.
[9] Now at Johns Hopkins University, Baltimore, MD 21218, USA.
[10] Researcher IIKW, Brussels, Belgium.

nonstatic conditions during the recording of holograms. In section 3, the layout of the holographic system is presented, which includes our modifications of the commercial holographic laser, the transport and monitoring of the laser beam, and the design of the dispersing lens. The synchronisation of the laser pulse with the neutrino beam pulse is briefly described. In section 4 follows an overview of our experience with the system during several months of running. Furthermore, preliminary results obtained during the replay of a small sample of holograms are given, which show that we achieved the expected resolution over a large volume. Section 5 contains a summary of our new developments and a brief outlook on further applications of the technique.

2. Theory and design considerations of the modified single-beam technique

A hologram is formed by the interference of coherent light from a reference beam with the coherent light scattered by objects. In our case the objects are vapour bubbles with a refractive index of ~ 1.0 in a liquid with an index of ~ 1.088.

In two small bubble chambers, operated with liquids above room temperature [1,2], an in-line, or Gabor-type, illumination was used: an expanded parallel laser beam passes through the liquid onto the holographic film. Only a small part of this beam is diffracted by the bubbles and interference between the diffused and non-diffused waves produces fringes which are recorded by the emulsion. For HOBC [2], two-beam geometries were tested, where the reference beam did not pass through the medium to be holographed. Due to the layout of our existing 15-Foot Bubble Chamber, having a volume

more than three orders of magnitude larger than that of the small chamber HOBC, we had to modify the standard holographic techniques.

We describe the experimental scheme (as used in the second physics run), in which the object and reference beam are combined in a new way. The laser beam enters the Bubble Chamber (fig. 1), filled with a 63/37 mol% Ne/H_2 mixture, at its bottom through a specially designed aspheric diverging lens, which also serves as an entrance window. This lens – a sophisticated beam splitter – is designed so that only a small part of the laser light goes through the liquid to a set of three concentric hemispherical windows (fish-eye lenses) on the opposite side of the Chamber directly onto the film. This reference beam exposes completely the 70 mm holographic film format. The rest of the beam illuminates the tracks within a conical volume. The intensity of this object beam is designed to increase at large angles to partly compensate for the decrease of the light scattered by the bubbles at these angles. Some elementary formulas, together with estimates based on experience in the smaller bubble chambers, are given in ref. [6]. The latter contains data on the optical resolution of such a system, the energy needed to illuminate a given volume, the ratio of intensities of object to reference beam, and the required resolution of the photographic emulsion. These data will be re-evaluated in the context of our recent experience. A large coherence length, and a Gaussian-like spatial distribution (TEM$_{00}$ mode) of the beam from the oscillator stage, together with a fairly uniform profile of the amplified laser beam over the aperture of the dispersing lens are important laser beam properties for our experiment.

In applying this modified single-beam technique to holography of tiny bubbles in a cryogenic multi-cubic-
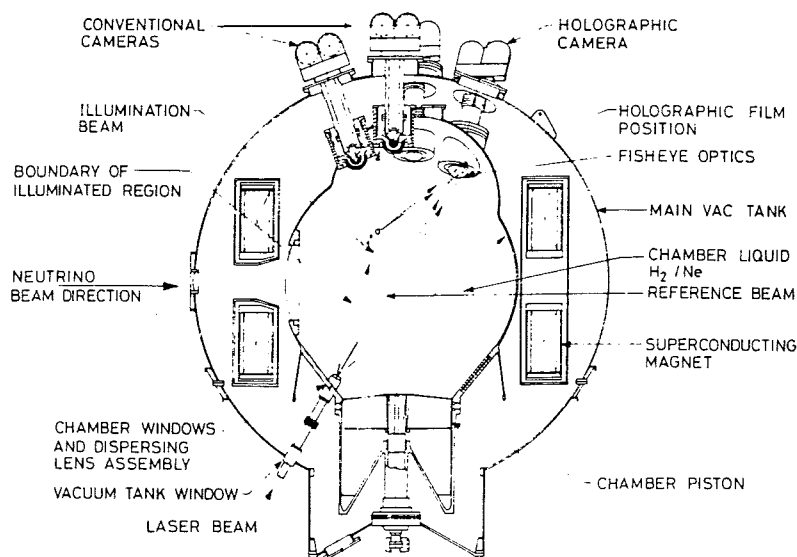

Fig. 1. 15-Foot Bubble Chamber, side view.

meter Bubble Chamber, several disturbing experimental effects had to be controlled. The most serious of these disturbances arise from:

a) excessive heating of the cryogenic liquid by the intense laser light, causing parasitic bubble creation and thereby unwanted scattered light;

b) vibration of the equipment during the mechanical expansion of the liquid; and

c) movement and growth of track bubbles during the laser illumination. Furthermore,

d) multiple scattering of the laser light from the Chamber wall, which is covered with a reflecting material (Scotchlite), can spoil the quality of the hologram, lower the contrast, and decrease the visible volume.

We give here some of the design considerations which govern the choices of laser energy, pulse length, and light distribution inside the Bubble Chamber needed to maximize the volume recorded in the hologram. These considerations also indicate hardware changes which help to achieve this goal.

2.1. Effect of background light (noise) hitting the holographic film

The information available to be recorded on the holographic film is the fringe pattern formed by the interference of the reference beam and the object beam (i.e. the light scattered by a bubble). Therefore, bubbles which give the same fringe modulation M and are at the same Θ_h (fig. 2), will be equally well recorded on the film and be equally bright in the replayed hologram.

We define the Beam Branching Ratio (BBR) as the intensity, on the holographic film, of the laser light scattered from a single bubble, divided by the reference beam intensity. The BBR in this application is given by the formula

$$BBR = \frac{F(\Theta_i) r^2 G(\alpha) \cos(\Theta_h)}{I_r d_i^2 d_f^2},$$
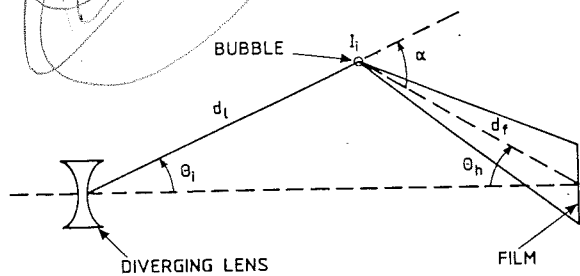

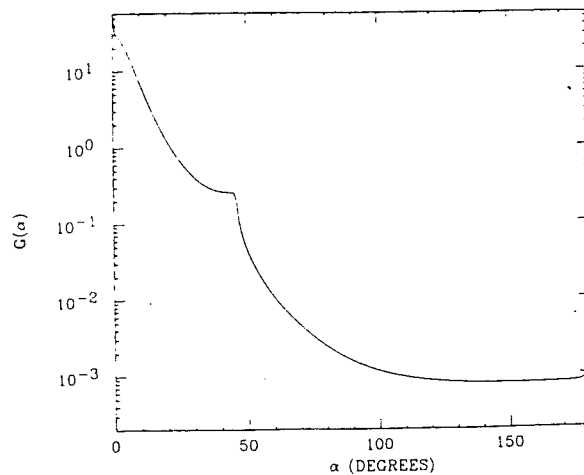Fig. 2. Simplified representation of the holographic setup with the holographic parameters.

Fig. 3. Geometric scattering function $G(\alpha)$ as function of the scattering angle α.

with (fig. 2)

r = bubble radius,

d_i = distance between the bubble and the dispersing lens,

d_f = distance between the bubble and the holographic film,

Θ_i = illumination angle,

α = scattering angle,

Θ_h = angle between the reference beam and the scattered beam from the bubble at the film,

I_r = reference beam intensity,

$F(\Theta_i)$ = illumination intensity distribution per solid angle,

$G(\alpha)$ = scattering function (fig. 3 [17]).

In the geometry described above, once the light output distribution from the dispersing lens is fixed by the shape of the lens and the spatial distribution of the input laser beam, the BBR is determined (for 100 μm bubbles) at every point in the illuminated volume of the Chamber, and this ratio can be taken over any area on the film. The output energy of the laser is then adjusted to give the proper exposure of the film. We define

I_r = E_r^2 = intensity on the film plane of the reference beam (from the dispersing lens),

I_b = E_b^2 = intensity on the film plane of the light scattered from a bubble,

$BBR = I_b/I_r$,

r = $(BBR)^{1/2} = |E_b|/|E_r|$,

I_x = maximum intensity on film plane (where E_r and E_b constructively interfere),

I_m = minimum intensity on film plane (where E_r and E_b destructively interfere),

M = $(I_x - I_m)/(I_x + I_m)$ = fringe modulation on film plane.

Assuming that $E_r \gg E_b$, then

$$I_x = (E_r + E_b)^2 = E_r^2 + 2E_rE_b,$$

$$I_m = (E_r - E_b)^2 = E_r^2 - 2E_rE_b,$$

$$M = 4E_rE_b/2E_r^2 = 2r.$$

If there are other sources of light hitting the film, this calculation must be modified. In our setup, background laser light (noise from, for example, multiple reflections off the Chamber walls) hitting the film will be proportional to the overall laser intensity and hence proportional to the reference beam intensity, $I_n = kI_r$. The intensity of the light on the film is now

$$I_r + I_n = I_r(1 + k),$$

and we must reduce the overall laser beam intensity to avoid overexposing the film. A new laser intensity of $1/(1 + k)$ times the original will give the same exposure on film:

$$I_{n'} = I_n/(1 + k),$$

$$I_{r'} = I_r/(1 + k),$$

then

$$I_{r'} + I_{n'} = (I_r + I_n)/(1 + k) = (1 + k)I_r/(1 + k) = I_r.$$

Proceeding as above, but including the noise intensity and using

$$I_{x'} = (E_{r'} + E_{b'})^2 + I_{n'},$$

etc. results in

$$M' = 2r/(1 + k),$$

and we see that the net effect of the noise is to reduce the fringe modulation. If the noise were equal to the reference beam ($k = 1$), the laser output must be lowered to one half the original energy and the fringe modulation has been reduced to one half the original value.

Defining BBR' ($= r'^2$) as the Beam Branching Ratio needed, with noise, to get the same fringe modulation as was obtained without noise:

$$M' = M,$$

$$2r'/(1 + k) = 2r,$$

$$r' = r(1 + k), \quad \text{or}$$

$$BBR' = BBR(1 + k)^2,$$

thus, the presence of noise requires a higher BBR to obtain the same fringe modulation. In case of noise equal to reference beam intensity, a four times higher BBR is needed.

We then assume that all bubbles whose fringe modulation M is higher than a certain limiting value will be visible in the replayed hologram. The dispersing lens shape was optimized to give the largest volume with a BBR of 0.33×10^{-7} or greater for the lowest light input. Assuming that this corresponds to the M for which a

bubble is just visible, adding noise light equal to the reference beam ($k = 1$) would then require at least a BBR of 1.33×10^{-7} for a bubble to be visible. Referring to fig. 4, one sees that such noise would drastically reduce the volume visible in the hologram.

One source of such noise could be multiple reflections of the laser light inside the Bubble Chamber. The magnitude of this effect can be estimated with a simple calculation: if 10 J of laser light is sent into the Bubble Chamber, the average light intensity on the Chamber walls is 20 μJ/cm^2. The holographic film is part of the wall and requires ~ 0.9 μJ/cm^2-laser light to give the desired density. The average noise light is ~ 20 times the intended point source reference beam, indicating a potential problem. During the first physics run, hologram quality was degraded if more than ~ 0.6 J of laser light was sent into the Bubble Chamber. To solve this problem, baffles were designed and installed on the Chamber walls for the second physics run. These baffles trapped and absorbed the laser light after it had crossed the Chamber once (section 4.1).

Another potential source of noise laser light hitting the film is the multiple reflections inside the dispersing lens. Of the ≤ 10 J going through this lens, only 36 μJ is intended to hit the film (area = 40 cm^2) as the reference beam. Any of this intense laser light multiple reflected in the dispersing lens and hitting the film would add to the exposure and must be counted as noise, because it is not part of the point source beam used to construct the hologram. To prevent this, the dispersing lens was designed to function also as the Bubble Chamber pressure window, eliminating two potentially reflecting surfaces; the shape of all the dispersing lens surfaces were carefully adjusted, with the aid of a ray tracing program, to make serious multiple reflections miss the film; light absorbing baffles were
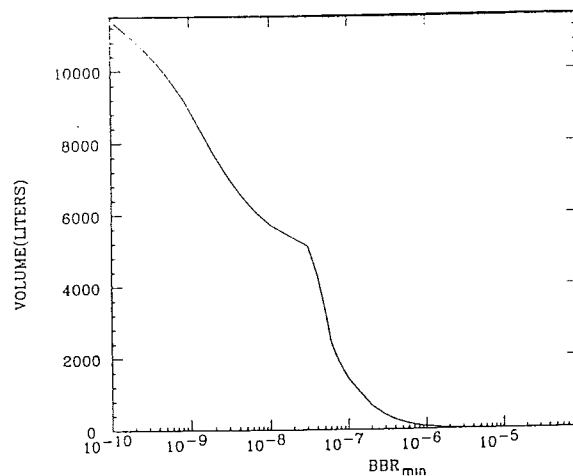

Fig. 4. Visible volume versus minimum detectable BBR in case no noise light is reaching the holographic emulsion.

placed between the lens elements and finally the surfaces in the laser beam were 'V'-antireflection-coated (sections 3.2 and 3.3).

When the Bubble Chamber was sensitive, the intense laser beam near the dispersing lens could induce bubble formation. Later in the laser pulse, these bubbles had grown large enough to scatter significant illumination light directly onto the film, becoming another source of noise laser light. Since this "microboiling" depends on the amount of microscopic particles (N_2 and H_2O) suspended in the Bubble Chamber liquid, this source of noise laser light proved very hard to control, and is thought to be responsible for much of the variation in hologram quality throughout the run. In order to reduce the laser beam intensity where it entered the Bubble Chamber liquid, the dispersing lens was designed so the output beam almost filled the 20-cm diameter of the lens (section 3.6).

2.2. Effects of bubble growth and movement, and vibrations during the laser pulse

As will be discussed in section 4.2, the need to prevent boiling of the Bubble Chamber liquid by the incident laser energy (≤ 10 J) necessitates the use of a "stretched" laser pulse ($\geq 1 \mu s$), rather than the more normally used Q-switched pulse (~ 30 ns), in order to minimize the instantaneous power flux in the pulse. This meant that, in principle, the effects of bubble growth and movement and of mechanical vibrations could cause a significant path length difference change between the reference and object beams during the laser pulse. The resulting changing phase between the two amplitudes reduces I_x and increases I_m giving a lower fringe modulation. We assume the phase changes linearly with time during the laser pulse, and we consider the desired "square wave" (i.e. intensity constant with time) laser pulse. Rewriting I_x (from the previous section) to include a phase angle β between E_r and E_b (where β varies during the duration of the laser pulse) $\Delta P/\lambda = $ instantaneous path length difference/wavelength,

$$\beta = 2\pi\Delta P/\lambda,$$

$$I_x = E_r^2 + 2E_r E_b \cos \beta.$$

I_x is then integrated over β from $-\delta$ to δ, choosing a central value of $\beta = 0$ to give the maximum intensity:

$$\bar{I}_x = E_r^2 + 2E_r E_b (\sin \delta)/\delta,$$

with a total path length difference change ($\Delta P/\lambda$) equal to δ/π from the beginning to the end of the laser pulse.

After I_m has been calculated in a similar manner, we find the fringe modulation

$$M' = 2r(\sin \delta)/\delta$$

has been multiplied by a factor $(\sin \delta)/\delta$, which is less than or equal to 1.0. Defining $BBR' (= r'^2)$ as the Beam Branching Ratio needed, with path difference change, to get the same fringe modulation as was obtained without this change:

$$M' = M,$$

$$2r'(\sin \delta)/\delta = 2r,$$

$$r' = r/(\sin \delta/\delta), \quad \text{or}$$

$$BBR' = BBR/(\sin \delta/\delta)^2.$$

For a path length difference change of $1/4\lambda$ ($\delta = \pi/4$), we require 1.23 times the BBR to get the same fringe modulation as we had without the change; this is a barely acceptable upper limit. If the change is limited to $1/8\lambda$, the factor is only 1.05 times the BBR.

Bubble diameters D grow according to $D = 2A\sqrt{t}$, where t is the time since growth started and A is a constant depending on the operating conditions (see section 4.2 for details). Assuming the Chamber is operated to grow our desired 100-μm bubbles in 1 ms, the bubble diameter is then growing at a rate of 0.1 μm/μs.

The optical path difference change for light scattered at an angle α off a bubble which has grown in diameter by ΔD is shown in fig. 5. For light which reflects off the bubble:

$$\Delta P = \Delta D n_1 \sin(\alpha/2),$$

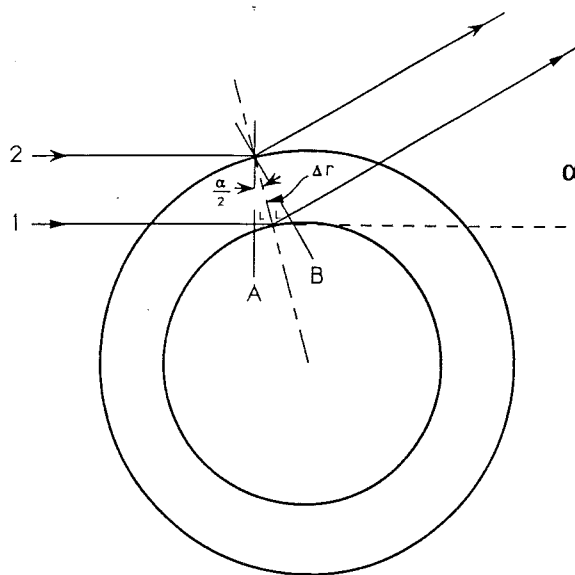where $n_1 = 1.088 = $ refractive index of liquid Ne/H_2.

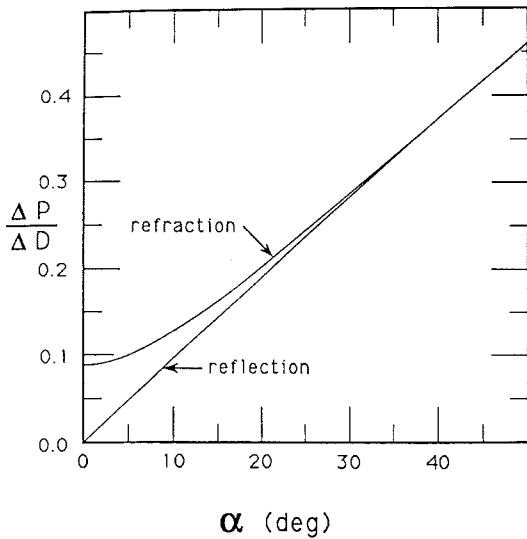Fig. 5. Optical path difference of growing bubble (schematic).

Fig. 6. Change in optical path length per change in diameter for a growing gas bubble in neon–hydrogen (liquid optical index 1.088) as a function of scattering angle α, for both refracted and reflected rays.

The expression for light refracting through the bubble is more complicated and will not be given here, but its value is shown in fig. 6 and agrees with the above expression within 5% for $\alpha > 23°$.

For a bubble with its diameter growing at 0.1 µm/µs, at an α of 30° (45°), the path difference change will be $1/4\lambda$ for a laser pulse length of 12.3 (8.3) µs. Laser pulse lengths of half these values would be required to limit the change in path length difference to the more desirable $1/8\lambda$.

During the first physics run, before this calculation had been made, most of the holograms were taken with 40-µs laser pulses and with higher bubble growth rates. This unfortunate choice clearly extracted a heavy penalty, both in the quality and in the volume of the Chamber that could be recorded in those holograms [11]. Laser pulse lengths of 7.5 µs or less were used during the second physics run.

Motion of the bubbles during the laser pulse has an effect similar to bubble growth. Track and bubble movement can be subdivided into two main categories: in their displacement together with the liquid due to its compressibility during expansion and recompression, and relative to the surrounding liquid, mainly due to buoyancy forces.

– The isentropic compressibility of our neon/hydrogen mixture is 1×10^{-3} cm^2 kg^{-1} [18]. The expansion ratio is $\Delta V / V \simeq 0.6\%$, V being the total liquid volume. The bubble movement together with the liquid is a function of the distance from the piston: it is more pronounced near the bottom of the Chamber than near the top. Furthermore, it depends upon the time when the tracks are produced: before the piston reaches its lowest position during expansion this displacement will be downwards, and during the recompression upwards. Since the beam is injected during the pressure minimum, when the piston is at its lowest position and almost at rest, we can neglect the bubble movement together with the liquid.

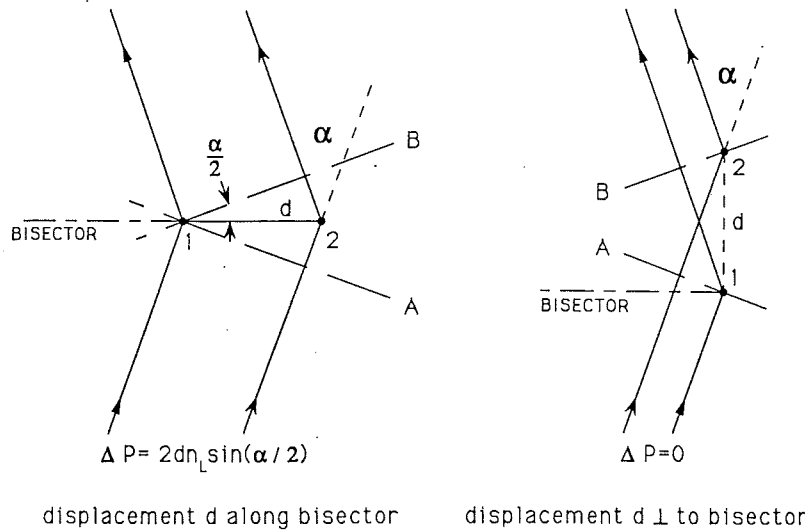– Theoretical predictions of the lift velocity of a bubble show only a slight dependence on temperature in the

Fig. 7. Optical path difference change of moving bubble.